ICES Journal of Marine Science

ICES Journal of Marine Science (2021), doi:10.1093/icesjms/fsab017

Application of a multibeam echosounder to document changes in animal movement and behaviour around a tidal turbine structure

Benjamin J. Williamson [1,2]*, Philippe Blondel[3], Laura D. Williamson [1,4], Beth E. Scott[2]

[1]*Environmental Research Institute, University of the Highlands and Islands (UHI), Thurso, UK*
[2]*School of Biological Sciences, University of Aberdeen, Aberdeen, UK*
[3]*Department of Physics, University of Bath, Bath, UK*
[4]*Ocean Science Consulting Limited, Dunbar, UK*

**Corresponding author: tel: +44 1847 889686; e-mail: benjamin.williamson@uhi.ac.uk*

Williamson, B. J., Blondel, P., Williamson, L. D., Scott, B. E. Application of a multibeam echosounder to document changes in animal movement and behaviour around a tidal turbine structure. – ICES Journal of Marine Science, doi:10.1093/icesjms/fsab017.

Received 26 October 2020; revised 9 January 2021; accepted 12 January 2021.

Changes in animal movement and behaviour at fine scales (tens of metres) in immediate proximity to tidal stream turbine structures are largely unknown and have implications for risks of animal collision with turbine blades. This study used upward-facing multibeam echosounder data to detect and track animal movement comprising fish, diving seabirds, and marine mammals. Measurements over spring-neap tidal cycles at a turbine structure (no blades present) are compared to a neighbouring reference area with no structure and comparable conditions, with measurements consecutive in time to maximize comparability.

The majority of tracked animals (93.4% around turbine structure and 99.1% without turbine structure) were observed swimming against the flow, with 87.5% and 97.8%, respectively, making ground and showing capability of manoeuvring in tidal stream flow speeds. Track tortuosity increased around the turbine structure compared to the reference site, particularly in the wake and at low flow speeds, indicating animal station-holding or milling behaviour. These data also evidence the benefits of multibeam echosounders to measure animal movement through larger measurement volumes rather than relying on single-beam echosounders to measure animal presence alone, including to avoid large biases overestimating the size of schools swimming against the flow measured by time-in-beam.

Keywords: Environmental monitoring; marine renewable energy; tidal stream turbines; fish behaviour; multibeam echosounder; target tracking

1. Introduction

Tidal stream turbines are contributing internationally to marine renewable energy generation (Smart and Noonan, 2018). In 2019, this corresponded to 10.4 MW of operating capacity in Europe (Collombet, 2020), with the MeyGen array in Scotland alone having generated over 31 GWh as of August 2020 (*SIMEC Atlantis Energy Annual Report*, 2019). Marine animals have been shown to use tidal-stream environments to increase foraging opportunities. For example, marine mammals (Hastie *et al.*, 2016) and diving seabirds (Waggitt *et al.*, 2016a) exploit high-energy hydrodynamic characteristics, which are hypothesized to increase foraging efficiency or prey availability (Benjamins *et al.*, 2015; Williamson *et al.*, 2019). However, despite widespread monitoring efforts often focusing on the fine-scale observations around turbines (Viehman and Zydlewski, 2015) or characterizing animal behaviour in tidal sites (Hastie *et al.*, 2019a), uncertainty remains

surrounding *changes* in animal behaviour around turbine structures at a scale of tens of metres (Benjamins *et al.*, 2015).

Species at risk from impacts vary between sites, often including fish, seabirds, and marine mammals. Common concerns include whether changes in behaviour around turbine structures will increase the risk of animal collision with rotating turbine blades, or change prey availability and predator foraging efficiency (Copping *et al.*, 2016).

1.1. Animal behaviour

Fish behaviour has been studied in the context of tidal turbines ranging from model turbines in tanks (Yoshida *et al.*, 2020) to presence (Hammar *et al.*, 2013; Broadhurst *et al.*, 2014; Kramer *et al.*, 2015; Viehman and Zydlewski, 2017), vertical distribution (Viehman *et al.*, 2015; Fraser *et al.*, 2018), behaviour and evasion (Amaral *et al.*, 2015; Viehman and Zydlewski, 2015; Bevelhimer *et al.*, 2016, 2017; Grippo *et al.*, 2017), school morphology, predator–prey interactions (Williamson *et al.*, 2017), and the predictability of fish behaviour (Williamson *et al.*, 2019). However, no study to date has investigated *changes* in the movement and behaviour of animals around a turbine structure compared to a reference location with comparable environmental conditions without a turbine structure, using deployments consecutive in time for comparability.

Changes in animal behaviour may arise from hydrodynamic effects such as the flow deficit and increased turbulence in a structure's wake (Fraser *et al.*, 2017a; Lieber *et al.*, 2019), or from visual or auditory perception (Benjamins *et al.*, 2015). Turbine structure effects on fish school behaviour have been shown in terms of increased abundance (Fraser *et al.*, 2018) and the predictability of abundance and changes to vertical distribution across tidal cycles and diel cycles (Viehman *et al.*, 2019; Williamson *et al.*, 2019).

Fish movement, although species- and site-dependent, is often linked to tidal flow. Fish may use selective tidal stream transport for movement and migration, or actively swim into the flow, holding station for energetic efficiency while foraging (Arnold *et al.*, 1994; Eloy, 2013). In tidal stream sites, small but significant differences in fish swimming direction and velocity have been shown between the presence and operation of a 5-m-diameter turbine (Bevelhimer *et al.*, 2017). Other studies have shown 5° to 20° differences in horizontal movement from the flow direction upstream of a turbine structure and increased variation in animal horizontal movement downstream, hypothesized to be a combination of upstream behavioural response and changes in the flow field downstream (Viehman *et al.*, 2017), yet these did not investigate the vertical movement and thus implications for prey availability and predator foraging. If these movements are repeated with every tidal cycle, and single devices are scaled up into arrays, then they are potentially significant in terms of energetics at individual and population levels.

Similarly, if changes in prey behaviour cause a change in the foraging behaviour of a predator, then this could cause changes in predator collision risk. Consideration of whether predators are diving or swimming against the flow (or *vice versa* moving with the flow) will affect both the perception of rotating blades and the time in the rotor-swept area (Wade *et al.*, 2012).

Recent studies observed that marine mammals often make use of tidally energetic locations for foraging and have examined the three-dimensional movement of harbour seals in tidal stream sites (Hastie *et al.*, 2019a). Measures of depth distribution, swimming direction relative to the flow, and vertical velocity were used to examine the use of a dynamic tidal environment with implications for the prediction of risk associated with interactions between diving seals and tidal turbines, although there were no turbines present (Hastie *et al.*, 2019a).

1.2. Hydroacoustic measurements

Optical measurements (cameras) are rarely used in isolation for measuring animal behaviour around tidal stream turbines, as turbidity limits effective range and adding illumination to extend monitoring to hours of darkness risks affecting animal behaviour. Instead, many studies use upward-facing multifrequency single or split-beam echosounders for a robust discrimination of marine animals in the turbulent environment of tidal stream sites where entrained air can compromise detection, e.g. Whitton *et al.* (2020), Fraser *et al.* (2017b), Scherelis *et al.* (2020). However, the relatively low sampling volume of single or split-beam echosounders limits their application to measure swimming speed, trajectory, or fine-scale movements around a turbine structure. Stationary single or split-beam echosounder school-size estimates are calculated based on the flow speed divided by the number of pings (time) a school is present in the echosounder beam (Fraser *et al.*, 2018), and thus when schools are present for longer in the beam due to swimming against the flow, they will be overestimated.

Other efforts use high-resolution, high-frequency (e.g. GHz) multibeam sonars (i.e. acoustic cameras) to track animal movement, e.g. Viehman and Zydlewski (2015) or Bevelhimer *et al.* (2017); however, these are limited to short sampled ranges of *ca.* 10 metres due to their high frequency and increased sound attenuation, and thus may not measure the entire water column or detect movements above and below the rotor-swept area. Lower-frequency (hundreds of kHz) multibeam echosounders provide greater ranges at lower resolution (Williamson *et al.*, 2016, 2017; Cotter *et al.*, 2017; Francisco and Sundberg, 2019; Hastie *et al.*, 2019a, 2019b).

In some cases, analysis of multibeam echosounder data is performed manually, which can be a time-consuming and subjective process (Viehman and Zydlewski, 2015). Other approaches have demonstrated automated detection (Bevelhimer *et al.*, 2017; Cotter *et al.*, 2017; Francisco and Sundberg, 2019; Hastie *et al.*, 2019a, 2019b). However, the performance of automated analysis remains variable under the dynamic and challenging conditions of tidal stream sites; manual inspection of data found that 74% of 181 unique tracks (individual fish and schools) were captured by automated analysis in one study, in peak currents up to 2.5 m/s (Bevelhimer *et al.*, 2017). Tracks not captured automatically were either too small, too weak, or only seen for two consecutive pings, highlighting the challenge of detecting individual fish as opposed to schools, which often provide a stronger return and a larger target. Other studies considering multiple target classes (fish, birds, seals, etc.) achieved a 58% true positive rate and a 99% true negative rate in peak currents up to 1.5 m/s (Cotter *et al.*, 2017).

1.3. Objectives

This study investigates whether animals exhibit significant changes in their movement around a tidal turbine structure (no nacelle or blades present). This study is testing the null hypothesis: H_0 *animal movement in a tidal energy site remains consistent*

around a tidal turbine structure. Specifically, movements at different ranges to the turbine structure on approach and departure, both upstream (i.e. during animal detection/perception of the turbine structure) and downstream (i.e. while the animal is in the structure wake), and at different depths. Additionally, this study investigates animal movement relative to flow, i.e. if animals are swimming with or against the flow with implications for under/overestimates (respectively) of school size if measured using single or split-beam echosounders alone (via time-in-beam). Animal movement relative to the flow has implications for potentially reducing or increasing collision risk, due to time spent in the rotor-swept areas, to inform future use of multi-sensor platforms for measurement and monitoring in these sites.

2. Methods

This study used a novel multi-instrument seabed platform with a multibeam echosounder to track the movement and behaviour of animals throughout the entire water column. The platform was capable of measuring animal proximity to a turbine structure and vertical evasion, and providing a fast update rate (7 Hz) capable of measuring animal movement, trajectory, and swim speed (Williamson *et al.*, 2017).

2.1. FLOWBEC platform and deployments

The *Flow, Water Column and Benthic Ecology 4-D* (FLOWBEC-4D) platform integrated multiple instruments to concurrently monitor the physical and ecological environment in marine energy sites (Williamson *et al.*, 2016). Onboard batteries and data storage provided a continuous recording of a 14-day spring/neap tidal cycle, and allowed measurements to be taken adjacent to marine energy structures and in areas free from such devices (Williamson *et al.*, 2017). Rapid (*ca.* 24-hour) servicing periods between successive deployments allowed recovery and redeployment fast enough that the environmental conditions had not significantly changed.

An Imagenex 837B Delta T multibeam echosounder (260 kHz, with a 120° × 20° vertical swath aligned with the tidal flow, sampling seven times per second with a range setting of 40 m, and an effective beamwidth of 0.75°) was synchronized with an upward-facing Simrad EK60 multifrequency (38, 120, 200 kHz, with a 7° beamwidth) scientific split-beam echosounder sampling once per second (Williamson *et al.*, 2017). The multibeam echosounder was not calibrated for this study; consequently, all backscatter measurements are considered relative, not absolute. The EK60 was calibrated using a 38.1-mm tungsten carbide sphere following the standard procedures (Foote *et al.*, 1987).

A SonTek/YSI ADVOcean 5 MHz Acoustic Doppler Velocimeter (ADV) was used for concurrent flow measurements for part of the deployment durations, mounted on the FLOWBEC platform with the sampling volume approximately 0.85 m above the seabed (Fraser *et al.*, 2017a). ADV measurements were extended to water-column velocity using 15-minute resolution outputs from a 3-D hydrodynamic model with 20 depth layers and a cell size of 100 × 100 m at the FLOWBEC platform deployment locations. The model was developed in Finite Volume Coastal Ocean Model (FVCOM) by FLOWBEC-4D project partners P. Cazenave and R. Torres at the Plymouth Marine Laboratory, UK, and verified to be in phase with onboard ADV measurements of velocity (Waggitt *et al.*, 2016b).

This study focuses on two consecutive deployments of the FLOWBEC platform (FoW1: 2 Jun—15 Jun 2013 comprising 12.35 days of data collection, and FoW2: 18 Jun—5 Jul 2013 comprising 17.05 days of data collection) at the European Marine Energy Centre (EMEC) Fall of Warness (FoW) tidal site in Orkney, Scotland (Figure 1) (Williamson *et al.*, 2016). A deployment 22 m from the centre of the Atlantis AK-1000 tidal turbine base (FoW1, Figure 2) is compared to a "reference" deployment, in similar conditions 424 m away in an area free from devices (FoW2). The turbine support structure included a 10-m-high piling and three 4-m-high ballast blocks; no nacelle or blades were present, and there were no opportunities to deploy adjacent to an operational tidal turbine. For reference, the blades for the AK-1000 turbine would be 18 m in diameter, with a rotor-swept height of approximately 4.5-22.5 m above the seabed.

The two sites had comparable characteristics, including depth (approximately 35 m), flow speeds (up to 4 m/s), substrate and topography (verified by remotely operated vehicle surveys), distance from shore, and natural hydrodynamic conditions (verified by hydrodynamic model outputs and ADV measurements) (Waggitt *et al.*, 2016a; Williamson *et al.*, 2016; Fraser *et al.*, 2017a). This minimized the effects of natural spatial variations and maximized spatial comparability, such that any difference observed between the two sites was likely to be related to the presence/absence of the turbine structure. Deployments were consecutive in time to maximize temporal comparability within the constraint of a single measurement platform and to minimize changes in fish abundance or the relative abundance of different species over the period of deployments (Williamson *et al.*, 2019).

The FLOWBEC platform, and thus the swath of the multibeam echosounder, was aligned with the predominant bidirectional flow direction at each location as far as possible (Figure 3 right). A misalignment of approximately 26° at FoW1 was caused by deployment constraints; cabled acoustic Doppler current profilers (ADCPs) were already present on the seabed in line with the turbine structure on the flood and ebb flow direction (Figure 3 left). The FLOWBEC platform was deployed a few metres further to the south-west, necessitating a slight northward rotation to ensure the turbine structure remained centred within the multibeam swath. Due to the dimensions of the turbine structure and the proximity of the FLOWBEC platform, measurements were still conducted in the structure wake (Fraser *et al.*, 2017a).

Whereas the multifrequency echosounder provides a uniform detection of targets irrespective of flow direction and target movement due to the symmetric circular (conical) beam, relying on volume backscatter strength and target size thresholds (Fraser *et al.*, 2017b), the multibeam echosounder relies on multiple observations of a target to establish a track. Hence, if the swath is out of alignment with the flow or predominant movement direction of targets, detection probability will be reduced. For this reason, to avoid a bias in measurements between FoW1 and FoW2, *relative* comparisons are made without bias, for example changes in movement and behaviour, but *absolute* comparisons are not made, for example between the number of targets detected using the multibeam at each site, instead relying on the multifrequency echosounder for these measurements (Williamson *et al.*, 2019). In effect, as will be seen in Section 2.2, absolute comparisons would also be limited by sidelobe interaction with the turbine structure slightly reducing the detection area at FoW1, and reducing the range of horizontal movement that can be detected—

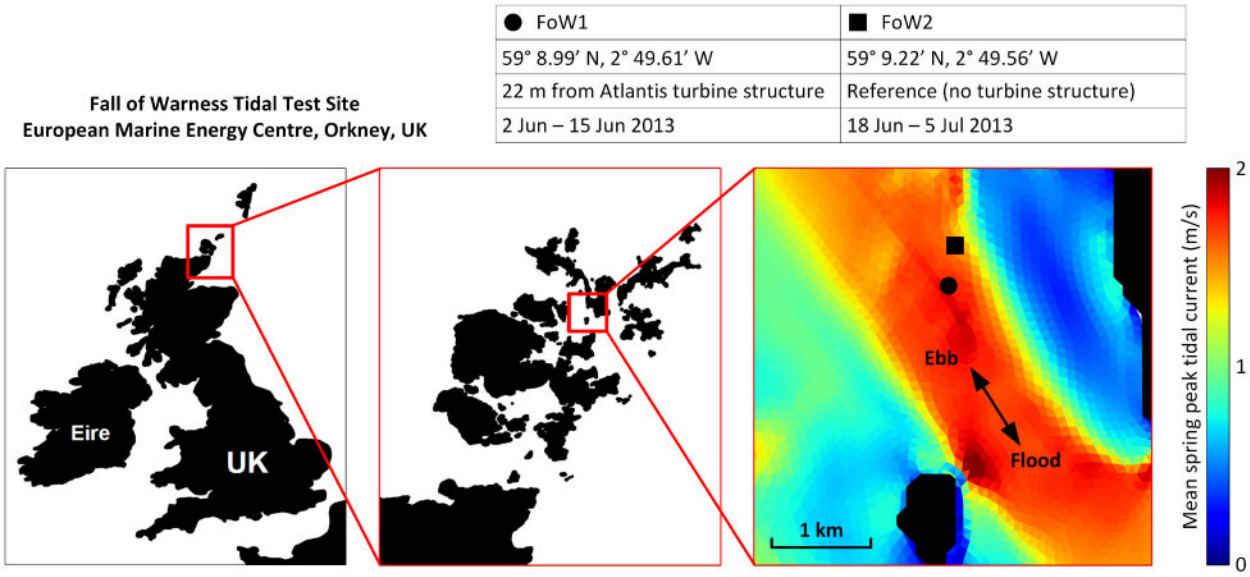

Figure 1. Two deployments of the FLOWBEC platform were used to investigate changes in animal movement and behaviour around a tidal turbine structure (FoW1) and in the absence of a turbine structure (FoW2). Figure adapted from (Williamson *et al.*, 2017). The map shows the mean spring peak tidal current, which is the mean of a 12-h period surrounding peak spring flow from hydrodynamic model outputs (Waggitt *et al.*, 2016b). Peak spring tides reach 4 m/s.

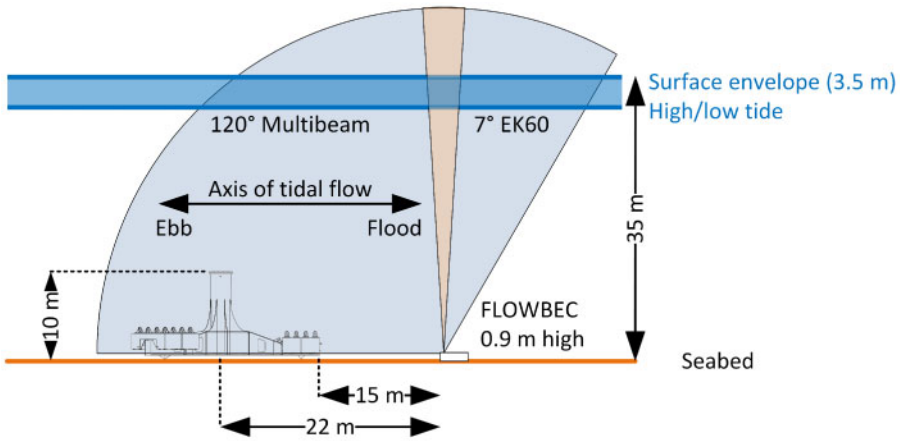

Figure 2. The FoW1 deployment was downstream of the Atlantis turbine structure during flood flow, approximately 22 m from the centre of the 10-m-high piling, and approximately 15 m from 4-m-high ballast blocks; no nacelle or blades were present. Figure adapted from (Williamson *et al.*, 2017).

hence, horizontal *speed* is used for comparison rather than the track length to avoid any bias.

2.2. Target detection and tracking

Multibeam echosounder data processing uses the following steps to process each dataset of approximately 8.4 million pings (14 days at 7 pings/second) and reduce it to useful target and track metrics.

(1) **Data pre-processing** to convert from proprietary raw transducer data (837 format) to beamformed data (83B format, 8-bit, 120 beams, 500 range bins) using manufacturer software Delta T software build v1.04.57 (Imagenex Technology Corp.), then imported into MATLAB R2019a (MathWorks). Data were acquired with a gain setting of 30 (arbitrary units), averaging disabled, a 240-µsecond pulse length, a range setting of 40 metres, and narrow-mixed beamwidth (0.75° beamwidth, with a 120° × 20° vertical swath).

(2) **Filtering** to mask background returns from the seabed and turbine structure, as well as reflections and "spoking" caused by transducer sidelobes, as previously documented (Williamson *et al.*, 2017). All filter parameters were tuned experimentally. The swath is cropped to 32 metres height (corresponding to 32.9 metres water depth) to reduce computation times unnecessarily devoted to measurements too close to the sea surface.

(a) A temporal median filter over 71 pings (ca. 10 seconds at 7 Hz) is used to generate a background mask

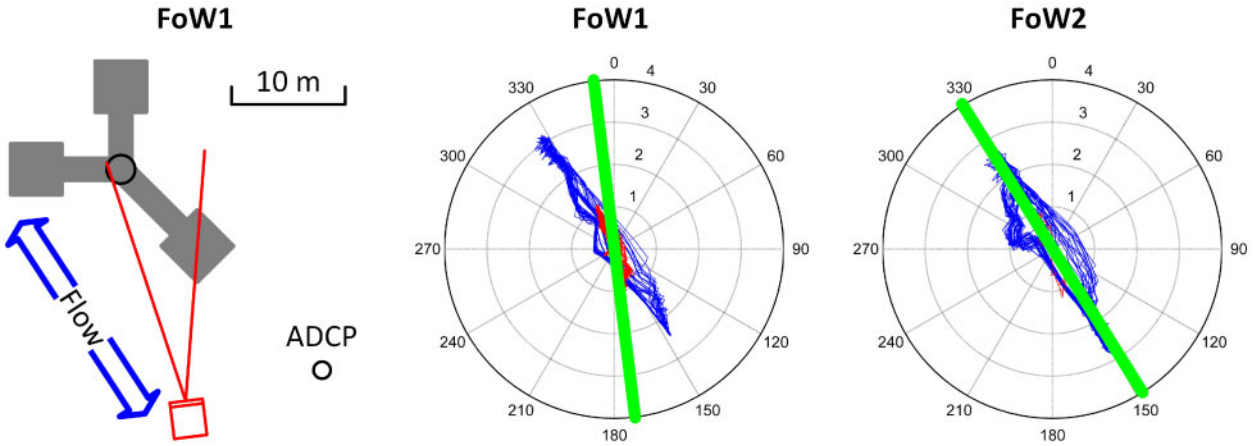

Figure 3. Right: the FLOWBEC platform (green line) was aligned with the flow direction as far as possible at each location, as measured by the ADV (red line) and depth mean of the hydrodynamic model (blue line) with flow speeds indicated on the radial scale (m/s). Left: a cabled seabed ADCP at FoW1 necessitated deployment out of position at FoW1, but still in the wake of the turbine structure as evidenced by ADV measurements, and still with the structure in the 20° swath (red lines).

providing an adaptive background subtraction for the conditions changing over time with, e.g., tidal flow. The data (and mask) are converted to Cartesian space by assigning each Cartesian pixel the value of the nearest-neighbour polar coordinate, where the resolution (pixel size) in Cartesian space is determined by the range resolution (0.08 m). The mask is dilated in Cartesian space using a disc-shaped structuring element of radius 15 pixels (1.2 metres).

(b) Morphological filtering in Cartesian space is also used to remove artefacts, noise, interference, reflections, and spurious returns, many of which may be specific to this model of multibeam echosounder: returns with an eccentricity > 0.95 corresponding to "lines" or very highly elongated ellipses, where an eccentricity of 1 is a line and 0 is a circle; returns with an area < 60 pixels; returns touching the edge of the multibeam swath. Although fine-scale measurements of size are approximate given the beamwidth and beam spacing, 60 pixels corresponds to an area of 0.38 m^2.

(c) A 3-D median filter is then applied in Cartesian space to de-clutter the data with dimensions $5 \times 5 \times 3$. 5×5 pixels correspond to spatial dimensions of 0.4 $\times$ 0.4 metres, and 3 pings is in the temporal context of 7 pings per second.

(3) **Target detection** is then used to parameterize all remaining water column returns as candidate targets, storing the pixel list of each return in each ping allowing it to be later extracted from the raw data, together with summary metrics of area, centroid, eccentricity, orientation, minimum/maximum intensity, and pixel sum (an alternative form of target strength, summing the arbitrary values of backscatter for all pixels comprising a target). An intensity threshold (arbitrary units, approximately corresponding to an acoustic backscattering threshold) is not applied and was deemed unnecessary, given the sensitivity of the already-thresholded 8-bit intensity beamformed data output from the Delta T software.

(4) **Target filtering** removes targets with a pixel sum < 200, corresponding to either very small or very weak returns. When multiple targets are detected within a ping, they are joined if within 75 pixels (6 metres) of each other—while this may appear conservative, it is used to link disjointed observations of the same target (e.g. multiple fish within a school, or multiple returns from a large target). The high flow conditions, high target speeds, and resolution and image quality of the multibeam echosounder necessitate this step, to avoid unnecessarily generating multiple tracked parts of the same target. As with other steps, this operation and threshold were validated using manual quality control (QC) and are deemed valid given the low occurrence of targets, particularly concurrent targets.

(5) **Target tracking** establishes correspondence between targets, aiming to identify the same target between successive pings to track the movement over time and space. The algorithm is a modified nearest-neighbour search (Williamson *et al.*, 2017), which seeks to establish a 1:1 relationship between all targets in the current ping to a maintained array of tracked targets (Thrun *et al.*, 2005). The closest (nearest-neighbour) target is selected as the corresponding target if its velocity is < 5 m/s between candidate observations, based on the typical maximum swim speed of species present at the site (AURORA Environmental Ltd, 2005). If there are multiple, equally-likely corresponding tracked targets, then the most recently observed tracked target is selected. Targets only need to be seen once to be considered as a track candidate, i.e. no voting-in (Thrun *et al.*, 2005), due to previous filtering. A list of tracked targets is maintained for 2 seconds in the case of non-detection, the equivalent of voting-out (Thrun *et al.*, 2005), to provide tolerance of temporary non-detections of a target. Target movement (e.g. across swath or changing attitude) and site conditions (e.g. entrained air, masking) may cause a target to be momentarily not observed. If a target is not observed for 2 seconds, it is assumed that the target has left the swath and the track is saved and closed. These values were tuned experimentally by inspecting

tracks under a variety of conditions to prevent mis-joined (false-positive) or disjointed (false-negative) tracks.

(6) **Track filtering** removes tracks of length < 5 observations to remove spurious noise, which has been incorrectly established as a track. This assumes that targets will be detectable in the multibeam swath for 5 or more pings, which was deemed valid given the 120° × 20° swath aligned approximately with the tidal flow and the typical swim speed of species present in the site (AURORA Environmental Ltd, 2005). Manual inspection of tracks under a range of conditions was used to verify this assumption.

(7) **Surface exclusion** is used to increase discrimination of ecological targets from entrained air near the sea surface. The sea surface is approximated as a horizontal line corresponding to the height of maximum backscatter in each ping and an additional 5-metre depth band mask applied to allow for the 20° across-track swath width, waves, and near-surface entrained air.

(8) **Manual QC** allows the user to review each track, remove any remaining false-positive tracks arising from persistent noise or interference, clean a track removing any incorrectly included returns or augment any missed returns as evaluated using manual scrutiny, and augment the start and end of a track when the target may fall below the automatic filtering thresholds.

Target tracks are stored allowing the reconstruction from raw data and parameterized by their minimum/mean/maximum values over time of the targets comprising a track, together with information on horizontal and vertical movements over ground, and horizontal and vertical movements relative to the surrounding water velocity. Metrics such as track tortuosity, speed, and changes in direction can then be derived.

Target movement relative to surrounding water velocity can be used to infer swimming behaviour, i.e. targets moving at speeds < the flow speed are assumed to be swimming into the current (head-upstream) and targets moving at speed > the current speed are assumed to be swimming with the flow (head-downstream).

Tracks were discriminated into individual animals or schools using morphology, i.e. detection of multiple simultaneous targets in a ping comprising a school. Further discrimination between individual animals (fish, diving seabirds, and mammals) was not applied. Following scrutiny in the QC process (step 8) to remove all false-positive tracks, the terms "target" and "animal" can then be used interchangeably, typically target or track when considering processing, and animal when considering behaviour.

The misalignment of swath and flow at FoW1 was not deemed to have impacted the results. Due to the wide swath width (20°) and the fast ping repetition rate (7 Hz), even if targets were moving with the flow (up to 26° off-axis to the swath), they would still be observed in enough pings for detection and to establish a track. For reference, the mean track lengths were 48.2 and 52.4 observations at FoW1 and FoW2, respectively, far higher than the minimum track length of 5 observations deemed necessary to establish a track.

2.3. Data analysis

The nonparametric two-sample Kolmogorov–Smirnov test was used to test for statistically significant differences between distributions of animal horizontal speed using a significance level $P < 0.05$. The modality of the probability density of distributions was estimated using Gaussian finite mixture models fitted via the expectation–maximization algorithm using the *mclust* package (Fraley *et al.*, 2012) in R version 3.5.1 (R Core Team, 2018). One- and two-proportion Z-tests were used to investigate the significance of differences in the proportion of targets in different movement categories, both within and between (e.g. FoW1 and FoW2) datasets using a significance level $P < 0.05$. Analysis of covariance (ANCOVA) was used to investigate significance of differences between animal movement relative to flow between FoW1 and FoW2 using a significance level $P < 0.05$.

Tortuosity (unitless) is calculated using the formula:

$$Tortuosity = \frac{Distance\ travelled}{Straight\ line\ distance}$$

Where the distance travelled is the sum of small distances a target moved between each observation in a track, and the straight-line distance is the difference between the first and the last observation of a target, i.e. the net target movement. Targets travelling in a straight line will have a tortuosity of 1.0, and targets travelling more tortuous paths will be associated with a value greater than 1.0 (Johnson and Moursund, 2000; Bevelhimer *et al.*, 2017).

3. Results

A total of 345 targets were tracked at FoW1 (turbine structure) and 541 at FoW2 (no turbine). All targets and tracks were verified by a manual inspection during the QC process. Tracks comprised individual animals (comprising fish, diving seabirds, and marine mammals) and schools of fish. Each track can be visualized in the context of the raw data (Figure 4 left), as movement over time (Figure 4 centre) and in the context of the flow velocity using outputs from the 3-D hydrodynamic model (Figure 4 right).

3.1. Target speed over ground

Distribution of animal horizontal speed over ground was significantly different ($P < 0.005$) between FoW1 and FoW2 (Figure 5). In the absence of the turbine structure (FoW2), animal horizontal movement was strongly bimodal, with peaks at -1.28 m/s and 1.68 m/s (Table S1) corresponding to movement left and right in the swath, respectively, and few targets moving at near-zero speeds (Figure 5). However, in the presence of the turbine structure, the distribution changed significantly with the peaks closer together, weighted more negatively (corresponding to moving towards the turbine structure), and with many more targets moving at a near-zero horizontal speed, with peaks at -1.14 m/s and 0.90 m/s corresponding to movement left (towards turbine) and right (from turbine) in the swath, respectively.

Vertical speed was centred around 0 m/s (Figure 5, Table S1), with minimal variance around this, showing that most targets maintained a vertical height as they passed through the swath. There were, of course, a few exceptions of targets that exhibited large vertical speeds, e.g. -1.36 m/s corresponding to a target that dived rapidly to the seabed.

3.2. Target speed relative to flow

The majority of targets at both FoW1 (93.4%, $X^2 = 257.3$, $P < 0.001$) and FoW2 (99.1%, $X^2 = 519.2$, $P < 0.001$) were observed swimming against the flow, even if not making progress

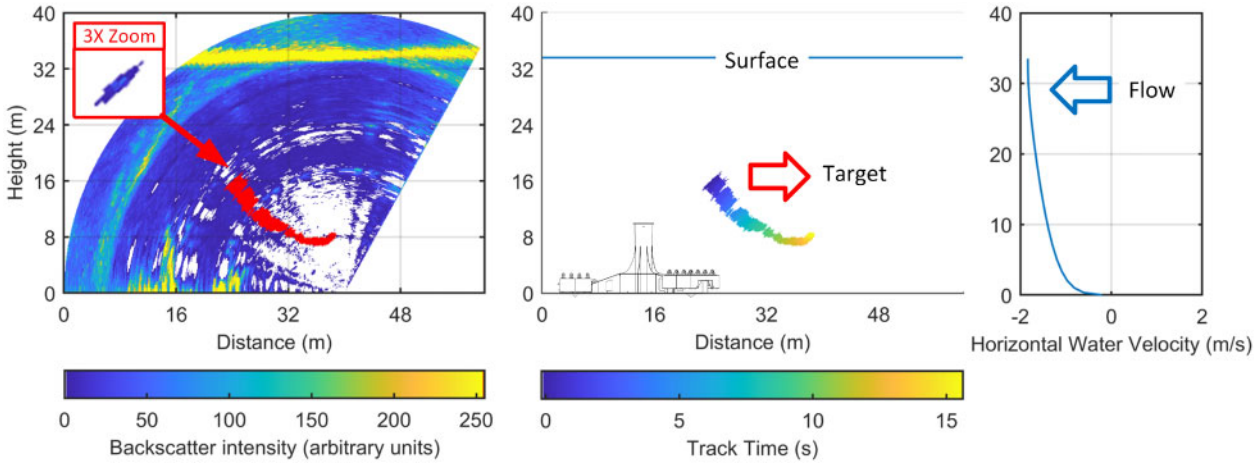

Figure 4. An example track output showing a diving target (left) with pixels tracked over 96 pings highlighted in red in the context of ±60 seconds of raw data. The zoomed inset (left) shows the raw target from the first ping comprising the track, with a maximum backscatter intensity of 68 (arbitrary units). The track can be visualized over time (centre, red arrow) actively swimming away from the turbine structure, against the flow (right, blue arrow).

over ground (Figure 6, Table 1). The lower target speeds over ground at FoW1 (Figure 5) occurred across flow speeds (i.e. targets were closer to the y-axis in Figure 6 for FoW1 than for FoW2, with a linear regression slope of -0.664 and -0.967, respectively, ANCOVA $P < 0.001$), showing slower movement over ground suggesting station-keeping or milling behaviour in the wake of the turbine structure. Apparent lower target speeds relative to the flow (targets making less ground swimming against the flow) at FoW1 may be amplified by the slower current in the structure wake, termed the "flow deficit" (Fraser *et al.*, 2017a), as this was not accounted for in the hydrodynamic model. For this reason, track tortuosity is later calculated (Figure 8) to further examine the potential for station-keeping or milling behaviour independently of flow speed or flow deficit.

More targets were detected at night around the turbine structure (72.5%) than at night in the absence of the structure (23.5%, $X^2 = 204.8$, $P < 0.001$) (Supplementary Material Figure S1 and Table S2), also highlighting the utility of the multibeam echosounder for detection irrespective of visibility. There was an increase in daytime targets swimming against the flow in the wake of the turbine structure (52.6% of daytime targets) compared to equivalent conditions in the absence of the turbine structure (35.3%, $X^2 = 9.1$, $P = 0.001$). This trend did not occur at night (64.0% compared to 67.7%, respectively, $X^2 = 0.4$, $P = 0.547$).

3.3. Vertical movement

Tracks of individual animals were split into movement towards (leftwards) and away from (rightwards) the turbine structure to investigate whether there was an observable range at which targets respond and change direction on approach, which could suggest a vertical evasion behaviour (Table 2). Individual animal tracks above a nominal 1 m/s turbine cut-in flow speed (Baston *et al.*, 2015) were generally horizontal, with little vertical movement or vertical variability (Figure S2). Instead, the greatest vertical variability occurred at flow speeds $\leq$ 1 m/s (Figure 7 by inspection), particularly for leftward targets approaching the turbine structure.

3.3.1. Tortuosity

Increased variability in the vertical movement of individual animals at FoW1 (Figure 7) can be quantified by an increase in track tortuosity, particularly at lower flow speeds (Figure 8). Track tortuosity increased at FoW1 compared to FoW2, particularly for targets detected during a positive flow speed (Figure 8). This indicates that individual animals moving in the turbine structure wake travelled more tortuous paths, predominantly against the flow, towards the turbine structure.

4. Discussion

This study has investigated the changes in animal movement around a turbine structure compared with a neighbouring reference location. Deployments were consecutive in time, 424 m apart, and under comparable physical conditions to minimize the effects of spatial and temporal heterogeneity in environmental conditions, and thus animal distributions and habitat use in tidal stream sites (Horne and Jacques, 2018; Viehman *et al.*, 2019). This study specifically quantified and compared the animal movement speed and direction (away from or towards a turbine structure, and with or against the flow), and whether animals changed depth, suggesting a vertical evasion or attraction/aggregation. These changes were investigated with the concurrent consideration of tidal and diel cycles to understand whether these changes in behaviour represent a change in habitat or habitat use.

Tracks included schools and individual animals (likely fish, diving seabirds, and mammals) and morphological thresholds were applied, including an area threshold of 60 pixels (corresponding to approximately 0.38 m^2) and a pixel sum threshold of 200 (arbitrary units). Hence, very small or very weakly backscattering targets were excluded, to ensure a robust target detection and tracking without false positives—all targets were verified using manual scrutiny during the QC process, and identical thresholds were used in both deployments to ensure the comparisons made within (e.g. flood/ebb) and between (e.g. turbine structure, no turbine structure) were robust.

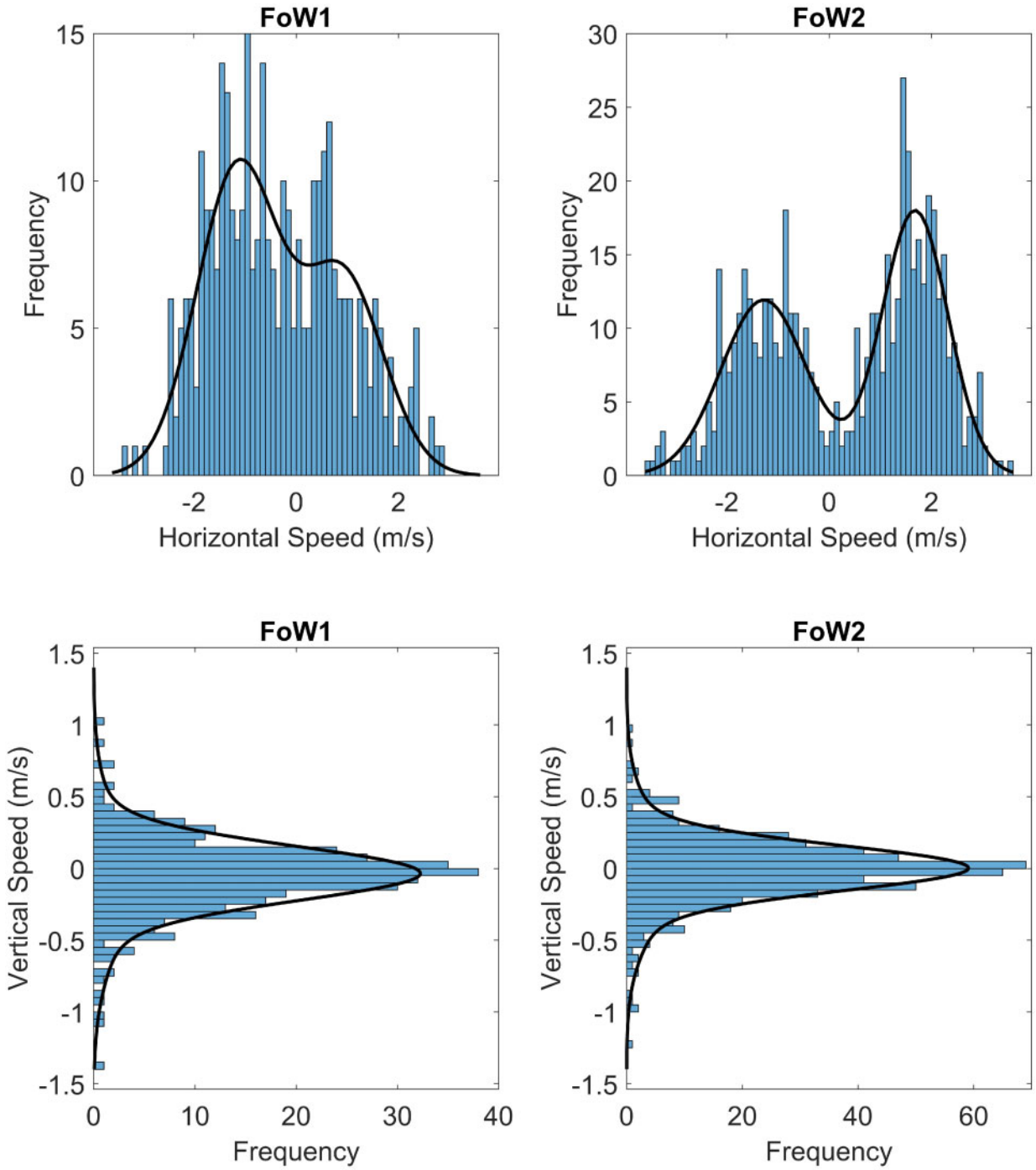

Figure 5. Horizontal and vertical target speeds over ground. Negative horizontal speeds at FoW1 indicate movement towards the turbine structure. Negative vertical speeds indicate downward movement. The probability densities of distributions estimated using Gaussian finite mixture models fitted via the expectation–maximization algorithm are shown.

4.1. Changes in behaviour

Animal horizontal speed over ground was bimodal in both the presence and absence of a turbine structure; however, around the turbine structure, the peaks were much less distinct with many more animals moving at near-zero horizontal speed. While the targets moving at high speeds through water were likely to be large individual animals, for example pursuit-diving seabirds and marine mammals known to forage in tidal stream sites (Waggitt *et al.*, 2016a; Hastie *et al.*, 2019a), the reduced bimodality in horizontal speed and increase in animal presence in the wake of the turbine structure concur with previous studies, which have observed an attraction/aggregation effect of a turbine structure on fish at low speeds (Kramer *et al.*, 2015), including particularly in the wake of turbine structures at this site (Broadhurst *et al.*, 2014; Williamson *et al.*, 2019). The mechanisms for this are suggested as a

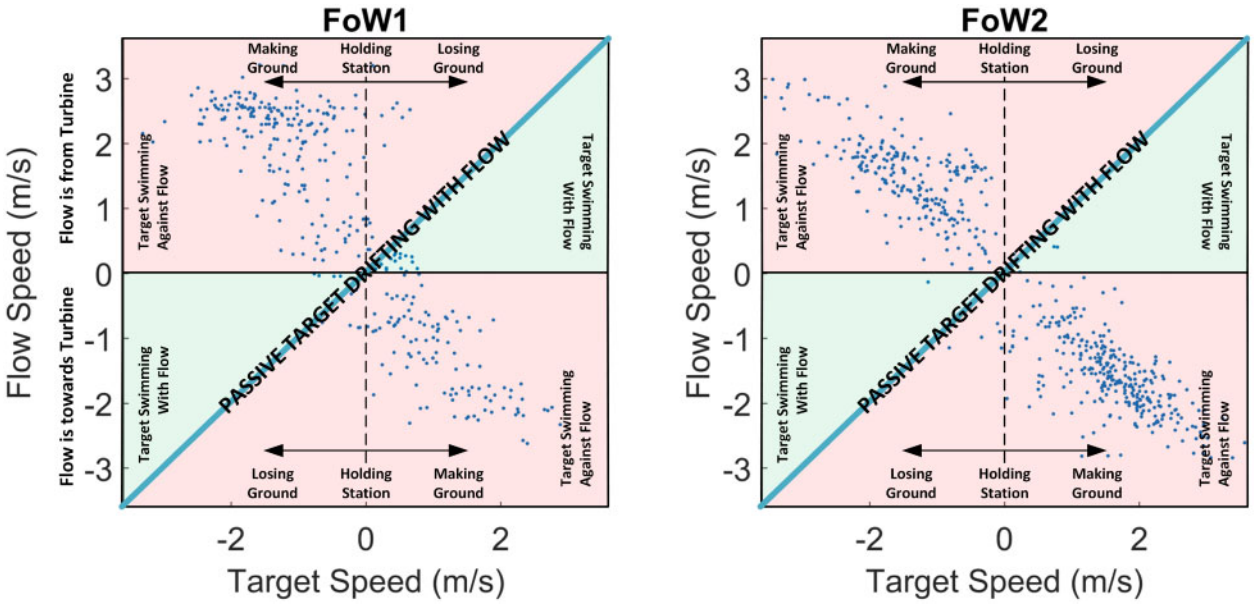

Figure 6. Target horizontal speed over ground relative to the instantaneous flow velocity at the target height for FoW1 (left) and FoW2 (right). Passive targets drifting with the flow will have a speed equal to flow speed (diagonal blue line). Targets swimming with the flow (green shading) have a greater target speed than flow speed. Targets swimming against the flow (red shading) can either be holding station (zero target speed over ground, despite a flow speed), or be making ground (target speed is opposite sign to flow speed), or be losing ground (target speed is the same sign as flow speed, but magnitude is lower). Positive flow speeds are flood tide (flow from the turbine structure at FoW1).

Table 1. Proportion of targets swimming with and against the flow during periods of flood and ebb (downstream and upstream of the turbine structure at FoW1, respectively).

	FoW1 (Turbine Structure)	FoW2 (No Structure)
Number of tracks	345	541
Flood targets against flow	60.9% (210)	42.9% (232)
Flood targets with flow	4.6% (16)	0.7% (4)
Ebb targets against flow	32.5% (112)	56.2% (304)
Ebb targets with flow	2.0% (7)	0.2% (1)

combination of refuge from predators or flow, enhanced foraging, or attraction to the structure (a fish-attracting device) (Boehlert and Gill, 2010).

4.2. Swimming against the flow

The majority of targets were observed swimming against the flow, even if not making progress over ground (Figure 6, Table 1). This is potentially linked to the mode of highest energetic efficiency for fish (Eloy (2013) and references within), and diving into the flow has been observed for seabird species foraging in tidal stream sites (Wade *et al.*, 2012). However, further investigation is needed to understand site specificity of marine mammal foraging behaviour with respect to flow speed (Hastie *et al.*, 2019a). This study assessed targets that likely included fish, diving birds, and mammals, which could be why the observed trend of swimming against the flow contrasts with results seen at other tidal stream sites, for example for small (10-20 cm length) fish (Viehman and Zydlewski, 2015, 2017) and harbour seals (Hastie *et al.*, 2019a).

The proportion of targets detected on the flood tide swimming against the flow in the wake of the turbine structure (60.9%) suggests animals attempting to hold station in the wake of the structure, for example for either energetic benefits (flow refuge) or anti-predation strategy (Higham *et al.*, 2015). This has two important implications.

First, the majority of targets (87.5% with the turbine structure and 97.8% without) were capable of making ground when swimming against the flow (Figure 6), suggesting a capability of manoeuvring in tidal stream flow speeds. This should be interpreted in the context of the mixed target classes and are likely to be strong swimmers, e.g. marine mammals such as harbour seals (Hastie *et al.*, 2019a), bottlenose dolphins (Rohr *et al.*, 2002), harbour porpoise (Sveegaard *et al.*, 2011), large fish, or diving seabirds (Wade *et al.*, 2012) known to be present in this site and capable of swim speeds greater than the flow speed (AURORA Environmental Ltd, 2005). However, the reduction in targets swimming against the flow in the ebb direction (56.2% compared to 32.5%) shows fewer targets were attempting to hold station upstream of the turbine structure (Figure 6, Table 1). If similar results are found at an operational turbine, this could increase the collision risk for targets swimming against the flow (93.4% of all targets around the turbine structure). This is not currently accounted for in the majority of collision risk models, as an

Table 2. Number and proportion of individual animals moving towards (leftwards) and away from (rightwards) the turbine structure, corresponding to Figure 7 (flow speeds ≤ 1 m/s) and Figure S2 (flow speeds > 1 m/s).

	FoW1 (Turbine Structure)	FoW2 (No Structure)
Number of individual animal tracks	179	396
Leftward tracks: Flow ≤ 1 m/s	12.8% (23)	9.6% (38)
Rightward tracks: Flow ≤ 1 m/s	17.9% (32)	7.8% (31)
Leftward tracks: Flow > 1 m/s	57.0% (102)	35.1% (139)
Rightward tracks: Flow > 1 m/s	12.3% (22)	47.5% (188)

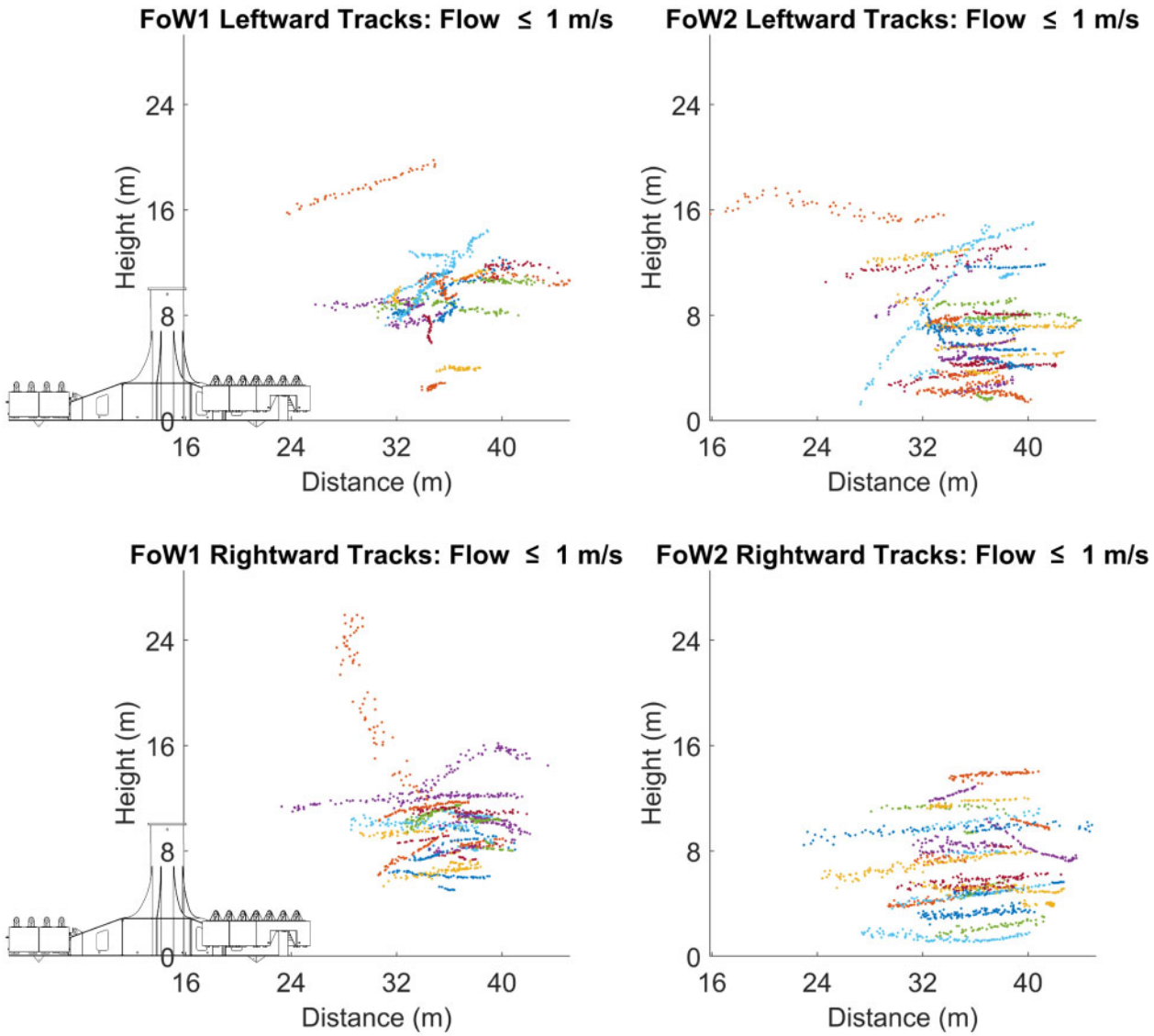

Figure 7. Individual animal tracks at flow speeds ≤ 1 m/s are shown for FoW1 (left column) and FoW2 (right column) distinguished by colour, split by animals moving leftwards (upper plots) and rightwards over ground (lower plots).

empirical measurement of swimming behaviour around turbine structures is largely unknown and highlights the importance of measuring the near-field evasion capabilities (Copping *et al.*, 2016). For example, predators have been shown to dive into the flow to maximize foraging efficiency, which may affect the perception of rotating blades (Wade *et al.*, 2012).

Second, the size of schools swimming against the flow will be overestimated by studies that just use the single- or split-beam echosounders, unable to measure the target movement (Viehman *et al.*, 2015; Shen *et al.*, 2016; Viehman and Zydlewski, 2017; Williamson *et al.*, 2019; Scherelis *et al.*, 2020; Whitton *et al.*, 2020). School-size calculation in conventional fisheries surveys

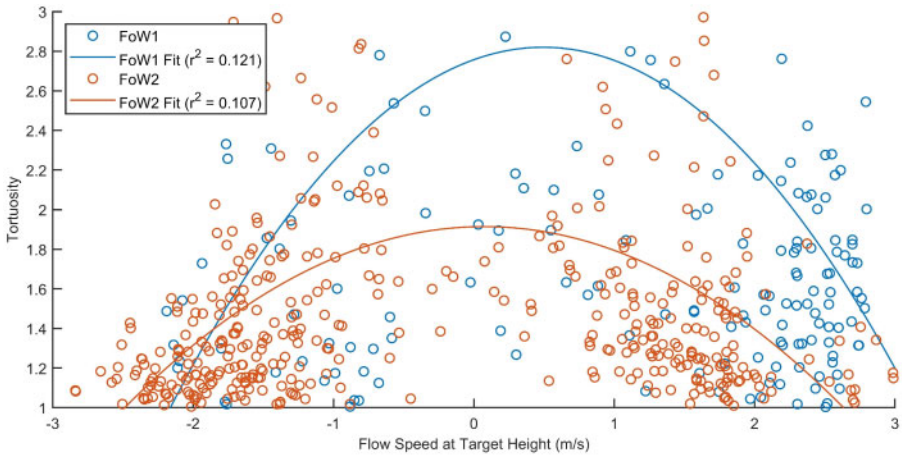

Figure 8. Tortuosity of individual animal tracks around the turbine structure (FoW1, blue) and in the absence of the structure (FoW2, orange) are shown against flow speed (positive flow speeds are flood tides, from the turbine structure at FoW1). A second-order polynomial is fitted to each dataset to investigate changes in tortuosity for leftward/rightward horizontal flow speed.

using a vessel-mounted single or split-beam echosounder assumes a vessel speed faster than any negligible fish swimming speed (Simmonds and MacLennan, 2005); however, this assumption is not valid for stationary seabed echosounders relying on a combination of flow speed and animal swimming behaviour to advect schools through the beam. Stationary single- or split-beam echosounder school-size estimates are calculated based on the flow speed divided by the number of pings (time) a school is present in the echosounder beam (Fraser *et al.*, 2018), and thus when schools are present for longer in the beam due to swimming against the flow, their size will be overestimated. These two implications highlight the importance of measuring animal swimming speed and movement with a multibeam echosounder, or similar (Williamson *et al.*, 2017).

More detections were observed at night around the turbine structure, with the opposite (more daytime detections) in the absence of a turbine structure (Figure S1 and Table S2). This increase in detections at night was seen in other studies at this location, which focused solely on fish schools (Williamson *et al.*, 2019). However, with the addition of tracking animal movement and behaviour using the multibeam sonar, this study has shown an increase in daytime targets swimming against the flow in the wake of the turbine structure compared to equivalent conditions in the absence of the turbine structure, which did not occur at night. This suggests visibility, or lack thereof, may be playing a role in behaviour near the turbine structure, potentially combined with diel variation in species assemblage.

4.3. Changes in movement around turbine structure

In the absence of a turbine structure, target movement was horizontal, with little vertical movement or variation. Occasional observations of tracks with large vertical movements across flow speeds or high horizontal speeds through water were likely to correspond to individual animals (seabirds and marine mammals) known to forage in these sites, in some cases diving to the seabed for foraging (Benjamins *et al.*, 2016; Chimienti *et al.*, 2017; Hastie *et al.*, 2019a); importantly for collision risk, these dives were observed across flow speeds and in the presence and absence of the turbine structure.

Increased vertical variation in target movement around the turbine structure at current speeds $\leq$ 1 m/s, particularly for targets moving towards the turbine structure in the low-speed wake (Figure 7), corresponds with targets holding a horizontal station (Figure 5), and with earlier studies showing an aggregating/attraction effect on fish schools in the low-speed structure wake (Williamson *et al.*, 2019). Future deployments around an operational turbine can be used to investigate the effect of rotating blades beyond the wake of the 10-m-high piling and three 4-m-high ballast blocks observed here (Fraser *et al.*, 2017a). This reduction in a vertical variation of target movement at higher flow speeds (Figure 7 and Figure 8) when combined with the tendency for animal movement against the current and making ground (Figure 6) may represent an important relationship between swimming ability, current speed, and the potential for turbine interactions and effects particularly above/below a threshold of 1 m/s. Further investigation of target classification will allow the investigation of whether this is a change in behaviour potentially combined with a different species assemblage at higher flows.

The increased track tortuosity of targets at a low flow speed in the structure wake (Figure 8) has also been observed in fish in other sites (Viehman and Zydlewski, 2015). Animals upstream may avoid being swept into the structure, and animals downstream may shelter in the structure wake. High tortuosity suggests animal station-holding or milling behaviour as seen elsewhere for fish (Johnson and Moursund, 2000; Viehman and Zydlewski, 2015); if this causes predators to swim into the flow, it may increase bottom time for diving predators, but if it increases foraging efficiency, it may reduce bottom time (Butler and Jones, 1997), with corresponding implications for predator collision risk. Diving into the flow has been observed in seabirds foraging in tidal stream sites (Wade *et al.*, 2012), although further studies are required to understand site and animal-specific foraging behaviour, e.g. for harbour seals (Hastie *et al.*, 2019a) or harbour porpoise (Johnston *et al.*, 2005; Gillespie *et al.*, 2020).

5. Conclusions

This study has shown significant changes in animal movement and behaviour around a tidal turbine structure. Animals were shown to swim against the flow, with station-holding or milling

behaviour in the wake of a turbine structure. This highlights the importance of using multi-sensor platforms incorporating multibeam echosounders to track animal movement rather than relying on single- or split-beam echosounders alone, including to avoid large biases in estimating school size and persistence for schools swimming against the flow, allowing ensonification of an entire school at once. The larger sampled volume, compared to single- and split-beam echosounders, allows simultaneous measurements throughout the water column for several tens of metres up/downstream to track animals on their approach and departure from a turbine structure providing unique insights into behaviour and interactions. Conversely, single- or split-beam echosounders may provide greater sensitivity, a calibrated measure of backscatter, and more robust discrimination of ecological targets from physical sources of backscatter, especially in the near-surface region (Fraser *et al.*, 2017b) when used in combination with multibeam echosounders (Williamson *et al.*, 2017).

If similar changes in animal movement and behaviour are seen around operational turbines, this may have implications for animal collision risk, energetics, and foraging efficiency. Similarly, diel differences in detection and animal movement have highlighted the importance of acoustic measurements over purely optical methods (cameras). Ongoing work is focused on robust target classification, augmented by other sensors where possible, to support further discrimination of individual animals (e.g. into fish, diving seabirds, and mammals) (Cotter and Polagye, 2020) to allow investigation of the implications of observed changes in movement for predator–prey interactions.

These techniques and results can be used to guide effective and proactive monitoring, regulatory, and management actions, if target tracking is shown to be effective around an operational turbine. They could also be used to trigger video data acquisition to confirm behaviours (such as evasion) and species identification when visibility and illumination permit. With a better understanding of changes in animal behaviour around individual turbines, arrays, and eventually multiple arrays, the predictive power of the outcomes of encounters from this type of research could lead to a wider strategic approach to monitoring, and a reduction in the level of monitoring required, to support the sustainable development of tidal energy.

Supplementary material

The following supplementary material is available at ICESJMS online: Table S1 shows the mean and standard deviation of horizontal and vertical target speed over ground corresponding to Figure 5 in the manuscript, together with the Gaussian finite mixture clusters for the bimodal horizontal speed. Figure S1 shows similar target speed relationships with flow between day and night at the two sites and Table S2 lists the proportion of targets in these diel categories. Figure S2 shows the individual animal tracks at flow speeds > 1 m/s.

Acknowledgements

We acknowledge the support of Shaun Fraser, Vladimir Nikora, James Waggitt, Paul Bell, Ian Davies, Eric Armstrong, and staff at Marine Scotland Science and the European Marine Energy Centre. Hydrodynamic model data were provided by Pierre Cazenave and Ricardo Torres (Plymouth Marine Laboratory). The constructive and extensive comments from three reviewers of an earlier version of this manuscript are gratefully acknowledged.

Funding

This work was funded by NERC and Defra (NE/J004308/1, NE/J004200/1, NE/J004332/1, NE/N01765X/1), a NERC MREKEP Internship, Innovate UK KTP (KTP009812), and the UK Department for Business, Energy and Industrial Strategy's offshore energy Strategic Environmental Assessment programme.

Data availability

The data underlying this article will be shared on reasonable request to the corresponding author.

References

Amaral, S. V., Bevelhimer, M. S., Čada, G. F., Giza, D. J., Jacobson, P. T., McMahon, B. J., and Pracheil, B. M. 2015. Evaluation of Behavior and Survival of Fish Exposed to an Axial-Flow Hydrokinetic Turbine. North American Journal of Fisheries Management, 35: 97–113. Taylor & Francis.

Arnold, G. P., Walker, M. G., Emerson, L. S., and Holford, B. H. 1994. Movements of cod (Gadus morhua L.) in relation to the tidal streams in the southern North Sea. ICES Journal of Marine Science, 51: 207–232.

AURORA Environmental Ltd. 2005. Environmental Statement. EMEC Tidal Test Facility Fall of Warness REP143-01-02,

Baston, S., Waldman, S., and Side, J. 2015. Modelling energy extraction in tidal flows, MASTS Position Paper.

Benjamins, S., Dale, A. C., Hastie, G. D., Waggitt, J. J., Lea, M., Scott, B. E., and Wilson, B. 2015. Confusion Reigns? A Review of Marine Megafauna Interactions with Tidal-Stream Environments. *In* Oceanography and Marine Biology, p 1–54.

Benjamins, S., Dale, A., van Geel, N., and Wilson, B. 2016. Riding the tide: use of a moving tidal-stream habitat by harbour porpoises. Marine Ecology Progress Series, 549: 275–288.

Bevelhimer, M., Colby, J., Adonizio, M., Tomichek, C., and Scherelis, C. 2016. Informing a Tidal Turbine Strike Probability Model through Characterization of Fish Behavioral Response using Multibeam Sonar Output. Oak Ridge National Laboratory (ORNL), Oak Ridge, TN (United States).

Bevelhimer, M., Scherelis, C., Colby, J., and Adonizio, M. 2017. Hydroacoustic Assessment of Behavioral Responses by Fish Passing Near an Operating Tidal Turbine in the East River, New York. Transactions of the American Fisheries Society, 146: 1028–1042. Taylor & Francis.

Boehlert, G. W., and Gill, A. B. 2010. Environmental and Ecological Effects of Ocean Renewable Energy Development: a Current Synthesis. Oceanography, 23: 68–81.

Broadhurst, M., Barr, S., and Orme, C. D. L. 2014. In-situ ecological interactions with a deployed tidal energy device; an observational pilot study. Ocean & Coastal Management, 99: 31–38.

Butler, P. J., and Jones, D. R. 1997. Physiology of diving of birds and mammals. Physiological Reviews, 77: 837–899. American Physiological Society Bethesda, MD.

Chimienti, M., Cornulier, T., Owen, E., Bolton, M., Davies, I. M., Travis, J. M. J., and Scott, B. E. 2017. Taking movement data to new depths: inferring prey availability and patch profitability from seabird foraging behavior. Ecology and Evolution, 7: 10252–10265.

Collombet, R. 2020. Ocean Energy - Key Trends and Statistics 2019, 24. pp.

Copping, A., Sather, N., Hanna, L., Whiting, J., Zydlewski, G., Staines, G., and Gill, A. 2016. Annex IV 2016 State of the Science Report: Environmental Effects of Marine Renewable Energy Development Around the World.

Cotter, E., Murphy, P., and Polagye, B. 2017. Benchmarking sensor fusion capabilities of an integrated instrumentation package. International Journal of Marine Energy, 20: 64–79.

Cotter, E., and Polagye, B. 2020. Automatic Classification of Biological Targets in a Tidal Channel using a Multibeam Sonar. Journal of Atmospheric and Oceanic Technology, 37: 1437–1455.

Eloy, C. 2013. On the best design for undulatory swimming. Journal of Fluid Mechanics, 717: 48–89. Cambridge University Press.

Foote, K. G., Knudsen, H. P., Vestnes, G., Maclennan, D. N., and Simmonds, E. J. 1987. Calibration of acoustic instruments for fish density estimation: a practical guide. ICES Cooperative Research Report, 144:

Fraley, C., Raftery, A. E., Murphy, T. B., and Scrucca, L. 2012. mclust Version 4 for R: Normal Mixture Modeling for Model-Based Clustering, Classification, and Density Estimation.

Francisco, F., and Sundberg, J. 2019. Detection of Visual Signatures of Marine Mammals and Fish within Marine Renewable Energy Farms using Multibeam Imaging Sonar. Journal of Marine Science and Engineering, 7: 22.

Fraser, S., Nikora, V., Williamson, B. J., and Scott, B. E. 2017a. Hydrodynamic Impacts of a Marine Renewable Energy Installation on the Benthic Boundary Layer in a Tidal Channel. Energy Procedia, 125: 250–259.

Fraser, S., Nikora, V., Williamson, B. J., and Scott, B. E. 2017b. Automatic active acoustic target detection in turbulent aquatic environments. Limnology and Oceanography: Methods, 15: 184–199.

Fraser, S., Williamson, B. J., Nikora, V., and Scott, B. E. 2018. Fish distributions in a tidal channel indicate the behavioural impact of a marine renewable energy installation. Energy Reports, 4: 65–69.

Gillespie, D., Palmer, L., Macaulay, J., Sparling, C., and Hastie, G. 2020. Passive acoustic methods for tracking the 3D movements of small cetaceans around marine structures. Plos One, 15: e0229058.Public Library of Science.

Grippo, M., Shen, H., Zydlewski, G., Rao, S. and Goodwin, A. 2017. Behavioral Responses of Fish to a Current-Based Hydrokinetic Turbine Under Multiple Operational Conditions: Final Report. 49 pp.

Hammar, L., Andersson, S., Eggertsen, L., Haglund, J., Gullström, M., Ehnberg, J., and Molander, S. 2013. Hydrokinetic Turbine Effects on Fish Swimming Behaviour. PLoS ONE, 8: e84141.Public Library of Science.

Hastie, G. D., Russell, D. J. F., Benjamins, S., Moss, S., Wilson, B., and Thompson, D. 2016. Dynamic habitat corridors for marine predators; intensive use of a coastal channel by harbour seals is modulated by tidal currents. Behavioral Ecology and Sociobiology, 70: 2161–2174.

Hastie, G. D., Bivins, M., Coram, A., Gordon, J., Jepp, P., MacAulay, J., Sparling, C., *et al.* 2019a. Three-dimensional movements of harbour seals in a tidally energetic channel: application of a novel sonar tracking system. Aquatic Conservation: Marine and Freshwater Ecosystems, 29: 564–575. John Wiley & Sons, Ltd.

Hastie, G. D., Wu, G.-M., Moss, S., Jepp, P., MacAulay, J., Lee, A., Sparling, C. E., *et al.* 2019b. Automated detection and tracking of marine mammals: a novel sonar tool for monitoring effects of marine industry. Aquatic Conservation: Marine and Freshwater Ecosystems, 29: 119–130. John Wiley & Sons, Ltd.

Higham, T. E., Stewart, W. J., and Wainwright, P. C. 2015. Turbulence, Temperature, and Turbidity: the Ecomechanics of Predator–Prey Interactions in Fishes. Integrative and Comparative Biology, 55: 6–20.

Horne, J. K., and Jacques, D. A. 2018. Determining representative ranges of point sensors in distributed networks. Environmental Monitoring and Assessment, 190:

Johnson, R. L., and Moursund, R. A. 2000. Evaluation of juvenile salmon behavior at Bonneville Dam, Columbia River, using a multibeam technique. Aquatic Living Resources, 13: 313–318.

Johnston, D. W., Westgate, A. J., and Read, A. J. 2005. Effects of fine-scale oceanographic features on the distribution and movements of harbour porpoises Phocoena phocoena in the Bay of Fundy. Marine Ecology Progress Series, 295: 279–293.

Kramer, S. H., Hamilton, C. D., Spencer, G. C., and Ogston, H. O. 2015. Evaluating the Potential for Marine and Hydrokinetic Devices to Act as Artificial Reefs or Fish Aggregating Devices, Based on Analysis of Surrogates in Tropical, Subtropical, and Temperate US West Coast and Hawaiian Coastal Waters. HT Harvey & Associates, Honolulu, HI (United States).

Lieber, L., Nimmo-Smith, W. A. M., Waggitt, J. J., and Kregting, L. 2019. Localised anthropogenic wake generates a predictable foraging hotspot for top predators. Communications Biology, 2:

Core Team R., 2018. R: A Language and Environment for Statistical Computing, R Foundation for Statistical Computing, Vienna, Austria.

Rohr, J. J., Fish, F. E., and Gilpatrick J. R, J. W.. 2002. Maximum swim speeds of captive and free-ranging delphinids: critical analysis of extraordinary performance. Marine Mammal Science, 18: 1–19. John Wiley & Sons, Ltd.

Scherelis, C., Penesis, I., Hemer, M. A., Cossu, R., Wright, J. T., and Guihen, D. 2020. Investigating biophysical linkages at tidal energy candidate sites; A case study for combining environmental assessment and resource characterisation. Renewable Energy, 159: 399–413.

Shen, H., Zydlewski, G. B., Viehman, H. A., and Staines, G. 2016. Estimating the probability of fish encountering a marine hydrokinetic device. Renewable Energy, 97: 746–756.

SIMEC Atlantis Energy Annual Report. 2019.

Simmonds, E. J., and MacLennan, D. N. 2005. Fisheries Acoustics: Theory and Practice. Blackwell Science.

Smart, G., and Noonan, M. 2018. Tidal Stream and Wave Energy Cost Reduction and Industrial Benefit: Summary Analysis. Report by ORE Catapult. 21 pp.

Sveegaard, S., Teilmann, J., Tougaard, J., Dietz, R., Mouritsen, K. N., Desportes, G., and Siebert, U. 2011. High-density areas for harbor porpoises (Phocoena phocoena) identified by satellite tracking. Marine Mammal Science, 27: 230–246. John Wiley & Sons, Ltd.

Thrun, S., Burgard, W., and Fox, D. 2005. Probabilistic Robotics. MIT, Cambridge, Mass.

Viehman, H., Hasselman, D., Boucher, T., Douglas, J., and Bennett, L. 2019. Integrating Hydroacoustic Approaches to Predict Fish Interactions with In-stream Tidal Turbines. FORCE Report, 300–208.

Viehman, H. A., Zydlewski, G. B., McCleave, J. D., and Staines, G. J. 2015. Using Hydroacoustics to Understand Fish Presence and Vertical Distribution in a Tidally Dynamic Region Targeted for Energy Extraction. Estuaries and Coasts. Springer US, 38: 215–226.

Viehman, H. A., and Zydlewski, G. B. 2015. Fish Interactions with a Commercial-Scale Tidal Energy Device in the. Natural Environment. Estuaries and Coasts, 38: 241–252. Springer US.

Viehman, H. A., and Zydlewski, G. B. 2017. Multi-scale temporal patterns in fish presence in a high-velocity tidal channel. PLoS ONE, 12: e0176405.

Viehman, H. A., Gnann, F., and Redden, A. 2017. Cape Sharp Tidal Gemini Multibeam Imaging Sonar: Monitoring Report (November 2016 - April 2017). Report to Cape Sharp Tidal. ACER Technical Report No. 123. 36 pp.

Wade, H. M., Masden, E. A., Jackson, A. C., and Furness, R. W. 2012. Which seabird species use high-velocity current flow environments? Investigating the potential effects of tidal-stream renewable energy developments. *In* BOU Marine Renewables and Birds.

Waggitt, J. J., Cazenave, P., Torres, R., Williamson, B. J., and Scott, B. E. 2016a. Quantifying pursuit diving seabirds' associations with fine-scale physical features in tidal stream environments. Journal of Applied Ecology, 23: 1653–1666.

Waggitt, J. J., Cazenave, P. W., Torres, R., Williamson, B. J., and Scott, B. E. 2016b. Predictable hydrodynamic conditions explain temporal variations in the density of benthic foraging seabirds in a tidal stream environment. ICES Journal of Marine Science: Journal du Conseil, 73: 2677–2686.

Whitton, T. A., Jackson, S. E., Hiddink, J. G., Scoulding, B., Bowers, D., Powell, B., Jackson, D., *et al.* 2020. Vertical migrations of fish schools determine overlap with a mobile tidal stream marine renewable energy device. Journal of Applied Ecology. John Wiley & Sons, Ltd, 57: 729–741.

Williamson, B. J., Blondel, P., Armstrong, E., Bell, P. S., Hall, C., Waggitt, J. J., and Scott, B. E. 2016. A Self-Contained Subsea Platform for Acoustic Monitoring of the Environment Around Marine Renewable Energy Devices – Field Deployments at Wave and Tidal Energy Sites in Orkney, Scotland. IEEE Journal of Oceanic Engineering, 41: 67–81.

Williamson, B. J., Fraser, S., Blondel, P., Bell, P. S., Waggitt, J. J., and Scott, B. E. 2017. Multisensor Acoustic Tracking of Fish and Seabird Behavior Around Tidal Turbine Structures in Scotland. IEEE Journal of Oceanic Engineering, 42: 948–965.

Williamson, B. J., Fraser, S., Williamson, L., Nikora, V., and Scott, B. 2019. Predictable changes in fish school characteristics due to a tidal turbine support structure. Renewable Energy, 141: 1092–1102.

Yoshida, T., Zhou, J., Park, S., Muto, H., and Kitazawa, D. 2020. Use of a model turbine to investigate the high striking risk of fish with tidal and oceanic current turbine blades under slow rotational speed. Sustainable Energy Technologies and Assessments, 37: 100634.

Handling editor: Olav Godø